Journal of
Scanning Probe Microscopy
Vol. 1, 55–62, 2006

RESEARCH ARTICLE

Strategies for the Deposition of Free Radical Organic Molecules for Scanning-Probe Microscopy Experiments

Wing-Tat Pong[1], Colm Durkan[1,*], Hongwei Li[1,2], and Wolfgang Harneit[3]

[1] Nanoscience Centre, University of Cambridge, 11. J J Thomson Ave, Cambridge, CB3 0FF, UK
[2] Chemistry Department, University of Cambridge, Lensfield Road, Cambridge, CB2 1EW, UK
[3] Physics Department, Free University, Arnimallee 14, D-14195 Berlin, Germany

In this article, we explore varieties of deposition methods of free radical organic molecules (i.e., molecules with unpaired electrons—single spins) for scanning tunneling microscopy (STM) and atomic-force microscopy (AFM) experiments. Free radical organic molecules BDPA (α,γ-bisdiphenylene-β-phenylallyl:benzene) were deposited by thermal evaporation, microcontact printing, and solvent deposition. We show that even under thermal evaporation, these molecules are undamaged and retain their unpaired electrons. We have deposited BDPA onto HOPG (highly oriented pyrolytic graphite) and Au(111) by thermal evaporation, and onto HOPG by microcontact printing and from solvent. BDPA tends to form micron-scale islands on HOPG, which are largely unsuitable for STM measurements, and 10 nm scale islands on Au(111) which are much more suitable. Such samples are ideal for single-spin detection experiments which are gaining increased interest in recent years.

Keywords: Atomic Force Microscopy, Scanning Tunneling Microscopy, Growth, Organic Molecules.

1. INTRODUCTION

It is now more than twenty years since the scanning tunneling microscope (STM) was invented. Scanning probe microscopy (SPM) techniques are nowadays common tools for characterising surface properties with spatial resolution down to the atomic level. STM can measure the surface topography and the local density of electronic states of conductive surfaces, and in recent years the territory of the STM has expanded into the magnetic domain. Spin-polarized STM[1] is a technique which is capable of mapping out the magnetic orientation of magnetic systems on a surface down to the atomic level. Using this technique, observations have been reported of domain walls[2] with a width of 0.6 nm and atomic scale anti-ferromagnetic structure.[3] Recent experiments by ourselves and others have indicated that it is also possible to detect single spins by tunnel current noise spectroscopy.[4,5] In the presence of an applied DC magnetic field B, the tunnel current which passes through or in the vicinity of an electron spin, with g-factor g, apparently becomes modulated at the Larmor frequency $g\mu_B B$, where μ_B is the Bohr magneton. Typical B-fields of 200 Gauss lead to a Larmor frequency of around 550 MHz, hence the need for high-speed detection. However, many open questions still remain regarding the use of this technique, which we would like to address systematically.[6] It is clear that reproducible experiments under tightly controlled conditions are needed to resolve these outstanding issues. Towards that goal, two critical steps must be taken: first, there must be appropriate STM hardware, with the capability of detecting low-amplitude high-frequency signals. We have reported the construction of such an STM elsewhere;[7] second, a suitable sample for unambiguous STM measurements. Free radical organic molecules are suitable candidates for these experiments as they contain unpaired electrons and thus provide electron spins.[8] The ideal sample should contain a mixture of singly-dispersed molecules as well as small clusters on a surface, rather than extended layers, so that we can probe single molecules and hence single spins. In order to facilitate our experiments on single electron spin detection by STM, we have explored three different methods (thermal evaporation, microcontact printing, solvent deposition) of depositing free radical organic molecules onto a substrate. Each deposition method has its own limitations which will be discussed later. Also a deposition method applicable to some kinds of molecules may not be applicable to others. Therefore, it is of tremendous help to widen up more

*Author to whom correspondence should be addressed.

 1557-7937/2006/1/055/008 doi:10.1166/jspm.2006.006

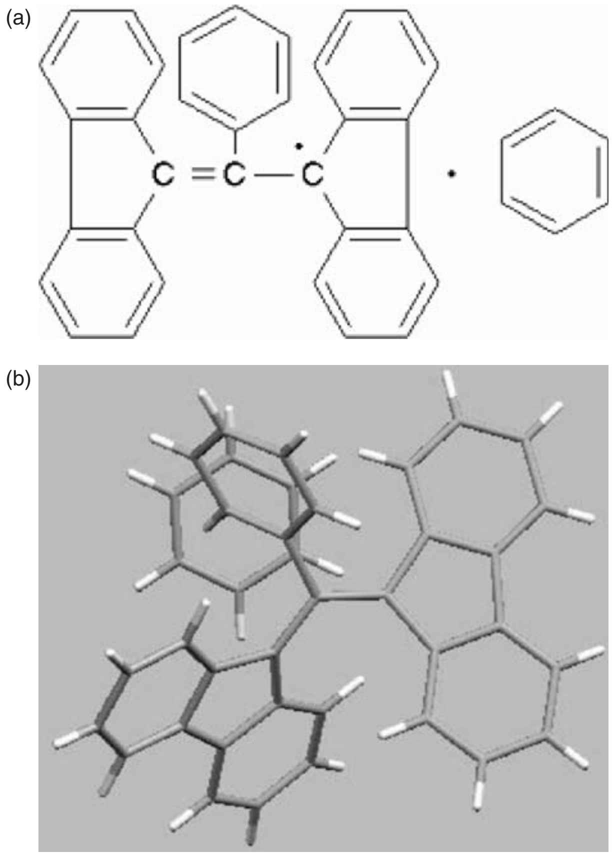

Fig. 1. (a) The structure of BDPA. (b) The 3D structure of BDPA.

deposition means so that an experiment need not be constrained by the restriction of a certain deposition method.

We have chosen a BDPA-benzene complex (α,γ-bisdiphenylene-β-phenylallyl:benzene)[9] as the material to deposit as it is a well-known spin label used in electron spin resonance (ESR) measurements. Also BDPA molecules are suitable for demonstrating all three deposition methods that we explore in this work. The chemical formula of BDPA is $C_{39}H_{28}$, with the structure as shown in Figures 1(a) and 1(b). The nominal size of a BDPA molecule is approximately 1.2 nm × 0.88 nm × 0.87 nm.

2. DEPOSITION EXPERIMENTS AND RESULTS

In principle, thermal evaporation/sublimation is the most desirable method of deposition, as samples can be prepared *in-situ* under UHV conditions and then imaged by STM without ever having to expose them to air. However, this method is not suitable for all free-radicals, hence the need to investigate alternative deposition methods.

2.1. Thermal Evaporation

We have deposited BDPA under high vacuum conditions (evaporator base pressure $\sim 10^{-8}$ mbar) as well as under UHV conditions (see later). Graphite was initially used as a substrate as it is easy to cleave to provide a fresh clean surface and it contains atomically flat terraces. The graphite was freshly cleaved by adhesive tape immediately before it was loaded into the vacuum chamber. We have deposited a 70 nm thick film onto a 5 mm × 5 mm graphite surface, at a deposition rate of ~0.05 nm/s as measured using a quartz crystal microbalance, by heating the BDPA to approximately 210 °C. The sample surface was then imaged by AFM operating in tapping-mode, under ambient conditions. In Figure 2(a), we can observe the bare graphite surface on the right which was masked during the evaporation process and the part deposited with 70 nm of BDPA on the left. The morphology of the BDPA in the AFM image is consistent with that observed by scanning electron microscopy (SEM) in Figure 2(b). Electron spin resonance (ESR) measurements were then performed on this sample in order to examine whether the heat of the evaporation process had damaged the structure and hence the spin property of the BDPA. Figure 3(a) shows a typical

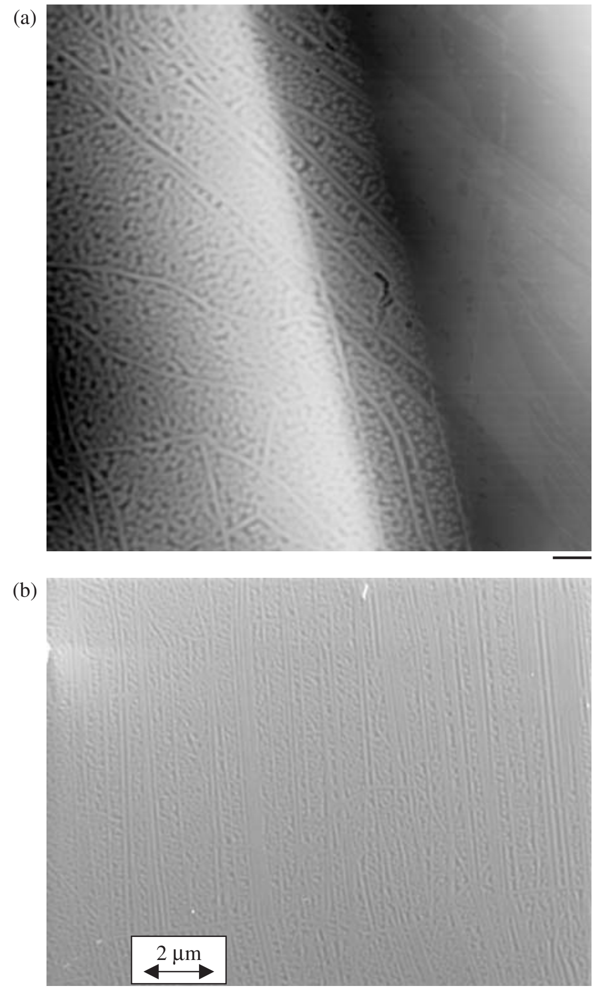

Fig. 2. (a) AFM tapping mode image, 20 μm × 20 μm, of BDPA evaporated on HOPG. The right hand side of this area was masked during evaporation, leaving the left side deposited with BDPA molecules. Scale bar is 1 μm. (b) SEM image on the part of the BDPA molecules on the HOPG surface.

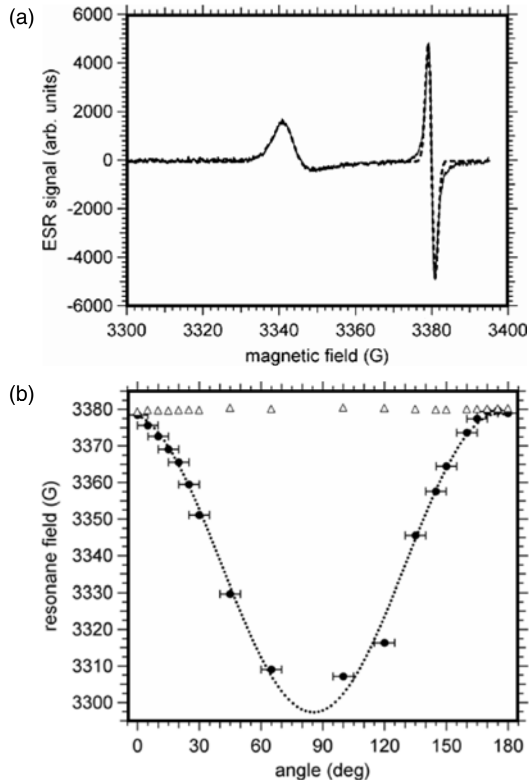

Fig. 3. (a) Solid curve: room temperature cw-ESR spectrum (X-band, 9.5 GHz) of a 70 nm thick BDPA film on HOPG. The surface normal was oriented at $\vartheta = 135°$ with respect to the magnetic field. Dotted line: fit with Dysonian profile[10] for the left peak which is due to HOPG conduction electrons, and with a Gaussian profile for the right peak due to BDPA. (b) Angular dependence of peak positions as obtained from fits similar to those shown in Figure 3(a). Open triangles: BDPA, no significant angular dependence. Solid circles: HOPG, the angular dependence can be described[9] by $B_0 - A\cos^2(\vartheta - \vartheta_0)$ with $B_0 = 3297.3(\pm 1.5)$ G, $\delta B = 81.6(\pm 1.9)$ G (dotted curve).

X-band ESR spectrum of the BDPA film on graphite. The surface normal was oriented at an angle of $\vartheta = 135° \pm 5°$ with respect to the external magnetic field B. The spectrum exhibits two lines, an asymmetric one crossing zero at $B = 3345.5$ G and a symmetric one at $B = 3380$ G. It is well known[10] that the conduction electrons of graphite give rise to an asymmetric peak in ESR measurements that can be described by Dyson's formula.[11] Due to the electronic anisotropy of graphite, the position of this peak has a characteristic angular dependence, as shown in Figure 3(b). We can thus assign the symmetric, angle-independent peak to the BDPA molecules. Taking the HOPG peak positions as an internal standard and assuming $g^{\mathrm{HOPG}} = 2.0026$,[10] we find a g-factor for BDPA $g^{\mathrm{BDPA}} = 2.0020$ (± 0.0005), which is a little smaller than the literature value of $g^{\mathrm{BDPA}} = 2.00359$.[12] In summary, the ESR measurements show that the spin signal of the BDPA molecules is preserved after the evaporation process, and therefore thermal evaporation provides a feasible way to deposit the free radical organic molecules for spin-based experiments. It should be pointed out that this is not definitive, as a 70 nm thick film is around 80 molecules thick, so we cannot be certain that a monolayer of molecules on a HOPG surface will retain its spin. We are reassured nonetheless that a thick film is essentially intact. We are limited by the spin sensitivity of ESR spectrometers which need around 10^{12}–10^{13} spins for a detectable signal, and a typical ESR resonator cannot accommodate a much larger sample than the one we have used. Future work will be to test this for film thicknesses down to one monolayer.

Having determined that evaporation does not destroy the BDPA molecules, we then prepared a number of samples with sub-monolayer thicknesses of BDPA on HOPG. From the AFM images in Figures 4(a) and 4(b) we observe that the BDPA molecules tend to aggregate together, forming islands ranging in size from around a few hundred nanometers to a micrometer with a tendency to decorate the step edges. The molecules appear to be highly mobile on the graphite surface and diffuse around until they either settle down along the step edges or attach to other molecules. The height cross-section in Figure 4(b) shows that the thickness of the islands is relatively even at around 0.486 nm, and given that the nominal height of BDPA molecules is approximately 0.88 nm, those islands are likely to be a monolayer high. The thickness of the islands is significantly smaller than the nominal height of a BDPA molecule, and such a discrepancy can be attributed to the fact that one of the atomic planes of a BDPA molecule is rotatable, and thus the actual height of the molecule on a surface depends on the interaction between the substrate and the molecule, and can be smaller than its nominal height. It is also possible that the AFM tip deforms the molecules during the imaging process, reducing their apparent height. We have not found any dependence of the apparent height on the imaging set-point (i.e., on the strength of the interaction between the AFM tip and the sample). As we shall see later, STM measurements of the molecular height on Au substrates show a similar value to that found by AFM, so it is more likely that the molecules undergo a conformational change whilst sitting on the surface. These molecular islands are relatively flat as opposed to the striated surface of the 70 nm thick BDPA film in Figure 2(a). This sample was imaged under AFM again after two months and the surface condition did not change noticeably over this period.

Repeated attempts at STM imaging of these evaporated samples however proved unsuccessful, even with a tunnel current as low as 2 pA and for tunnel gap voltages up to 1350 mV. We concluded that this is due to (i) the low conductivity of both the HOPG (being a semi-metal) and the molecules, as the STM tip is rather closer to that surface than for a metal and (ii) the greater diffusivity of the molecules on HOPG, as evidenced from the AFM images. As the molecular islands are extremely large, the tip has to penetrate the molecular layer in order for a measurable current to flow, so the molecules are moved out of the way by the STM tip during scanning.

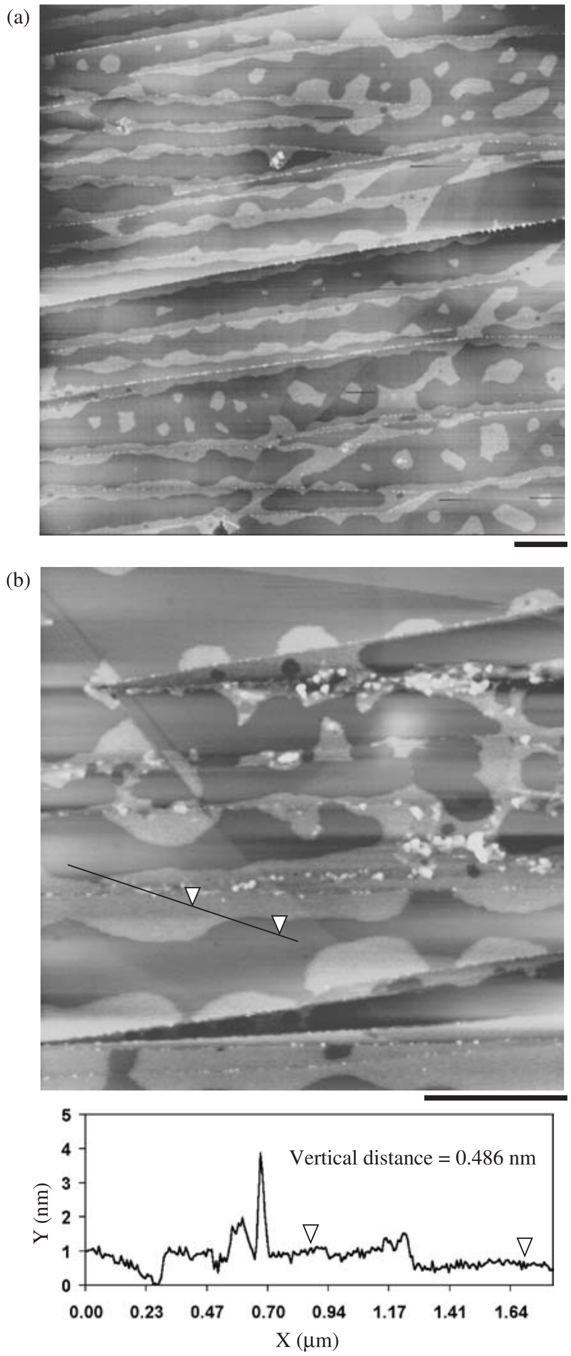

Fig. 4. (a) AFM tapping mode image, 11 μm × 11 μm, on the monolayer of BDPA molecules evaporated onto HOPG. Scale bar = 1 μm. (b) AFM tapping mode image, 3.8 μm × 3.8 μm, on the monolayer of BDPA molecules evaporated onto HOPG. The cross-section along the island shows its thickness to be approximately 0.486 nm which is a monolayer. Scale bar = 1 μm.

For STM imaging, small scattered islands of molecules are preferred as the scan range of STM is usually limited to within a few micrometers. As the distribution of the molecules is intimately related to the nature of the molecule–substrate and molecule–molecule interactions, we also investigated the use of the gold (111) surface[13] as a substrate. We used gold on mica which was annealed *in-situ* (in the UHV chamber containing the STM) at 380 °C for an hour to clean the surface. The gold was left to cool down for 30 minutes. Using a K-Cell operating at 210 °C, we then deposited approximately 0.2–0.3 monolayers of BDPA onto the Au(111) surface and transferred it into the STM. The base pressure of the STM chamber is $\sim 5 \times 10^{-10}$ mbar, although the chamber pressure goes up to around 10^{-7} mbar during BDPA deposition. This sample was then imaged with a tunnel current of 20 pA. From Figures 5(a–c) we can see that the molecules have scattered very well on the surface, and they form small, monolayer-high islands of tens of nanometres in size, ten times smaller than those on the graphite (cf. Figs. 4(a) and 4(b)), as well as smaller clusters of only a few molecules (single molecules are visible on the right-hand side of Fig. 5(b)). In-between taking images 5(b) and 5(c), the STM tip was used to manipulate several molecules out of the way. The BDPA molecules tend not to diffuse very far, and stay on the Au(111) surface without decorating the terrace edges. We can observe that there are many small pits on the Au(111) surface (Fig. 5(a)) which anchor the molecules onto the surface and prevent them from diffusing far. The effective diffusion length of BDPA on Au(111) is therefore around 10 nm, as compared to around 500 nm for HOPG. The thickness of the islands observed by STM is 0.4 nm, similar to that observed by AFM. Whilst STM does not give accurate topographic information for adsorbed species, the correspondence between the measured thickness by STM (0.4 nm) and by AFM (0.486 nm) is consistent with the idea that the BDPA molecules are physically deformed on the substrate surfaces. The molecules on the surface are rather stable, as the sample was imaged by STM again after two months, and no obvious differences were found. As expected, the substrate plays an important role in the deposition result as we have seen that the behaviour of BDPA on the Au(111) surface is very different from that on graphite. Au(111) surfaces are relatively more suitable substrates for depositing BDPA free radicals.

A further point worth mentioning regarding the deposition of BDPA on the Au(111) surface is that in our experiment, subsequent to the deposition we have observed gold stripes (gold fingers) along the terrace step edges (Figs. 6(a) and 6(b)). These gold stripe structures, not as well-known as the herringbone reconstruction, have been reported previously.[13–16] It has been proposed that these stripe structures are due to atomic diffusion induced by the STM tip operating with a strong local electric field.[15,16] The electric field enhances the atomic mobility on the Au(111) surface. The diffusion rate, R is governed by the Arrhenius equation,

$$R = \upsilon \exp(-E/k_B T) \tag{1}$$

where υ is the vibrational frequency of a surface atom, E is the activation energy, k_B is the Boltzmann constant, and T is the temperature.[15] Previous works produced the striped

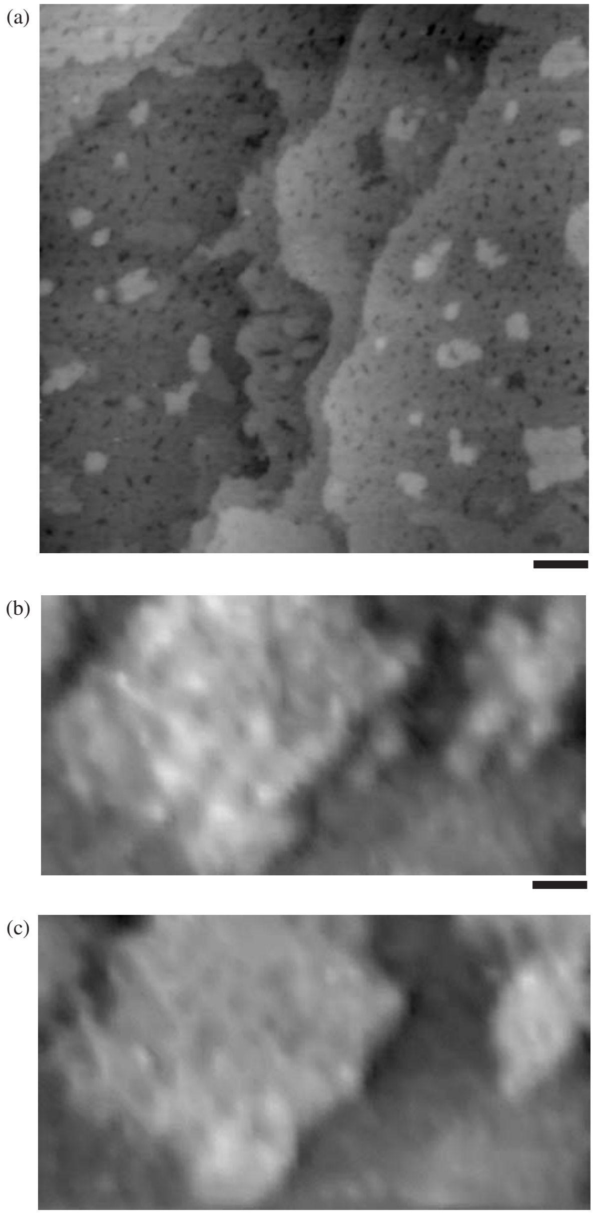

Fig. 5. (a) STM image of BDPA islands on Au(111). 200 nm × 200 nm, $I = 20$ pA, $V_{sample} = -850$ mV. Scale bar = 20 nm. (b, c) STM images of BDPA islands on Au(111). 50 nm × 26 nm, $I = 20$ pA, $V_{sample} = -800$ mV. Single molecules can be seen, particularly over on the right hand island, where the tip has moved some molecules away in between the acquisition of the two images. Scale bar = 10 nm.

structures by applying a high electric field with the STM tip. However, in our case, we did not apply a high electric field to deliberately induce the gold stripes. In fact, the tunneling conditions we used were 10–20 pA and 500 mV, which would produce a much weaker electric field than the electric field for the tunnelling conditions of 30 nA and 1.5 V as used by Guo et al.[16] Such a low electric field is unlikely to lower the activation energy E enough to accentuate the diffusion process. We believe that the activation energy has in fact been reduced by the molecules, as the molecule-surface interaction alters the surface energy. This

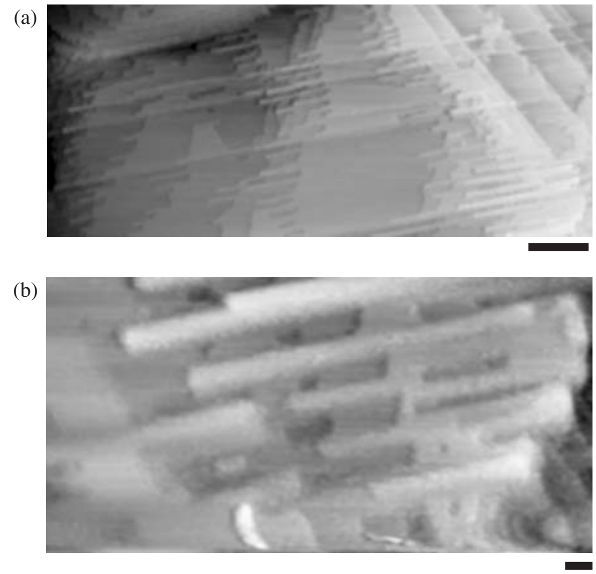

Fig. 6. (a) Gold stripe structures along the terrace step edges. 900 nm × 450 nm, $I = 10$ pA, $V_{sample} = 800$ mV. Scale bar = 100 nm. (b) A zoom-in of the gold stripe structure. 200 nm × 100 nm, $I = 50$ pA, $V_{sample} = 800$ mV. Scale bar = 10 nm.

is consistent with the deformation of the molecules which we are proposing, i.e., there is a strong molecule-surface interaction. Similar effects have been reported before for Lander molecules on the Cu(110) surface.[17]

2.2. Microcontact Printing (μCP)

Microcontact printing is a powerful technique for printing structures in the nanoscale to the microscale.[18] It uses a poly(dimethylsiloxane) (PDMS) stamp to deposit molecules onto a surface in predetermined patterns. The stamp is made by replicating structures on a solid master by molding with liquid prepolymer. The stamp is then inked with a solution of molecules such as proteins or alkanethiols which are to be coated onto the surface of a substrate. The stamp is dried, pressed into conformal contact with the substrate, and the molecules are printed onto the surface. Complex surface patterns of more than one kind of molecule are possible by repeated printing with different stamps. In addition to molecules, colloidal particles can also be printed by microcontact printing. Microcontact printing has many applications such as protein patterning,[18] polymer growth,[19] microelectrode arrays,[20,21] organic light-emitting diodes (OLEDs),[22] and organic thin-film transistors.[23] However, microcontact printing has the problem of surface diffusion which leads to edge disorders in the resulting patterns.

The procedure of microcontact printing consists of a number of steps (Fig. 7). First of all, a silicon master is fabricated by photo- or e-beam lithography. Then PDMS prepolymer is cast onto the solid master to make an elastomeric stamp. After the crosslinking of the PDMS, the elastomeric stamp is peeled off with the inverse structures of the master. The stamp is then immersed into the

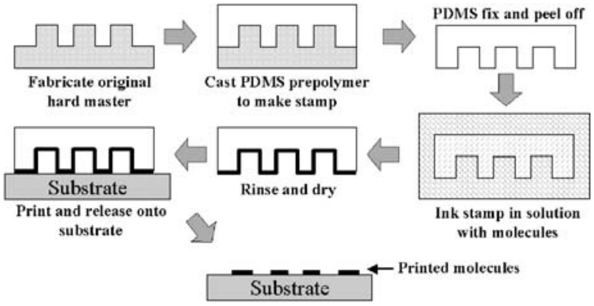

Fig. 7. The procedure of microcontact printing.

molecular solution. The stamp is then rinsed and dried, and a conformal contact is formed between the substrate and the stamp in order to transfer the pattern of the molecules onto the substrate surface.

In our experiment, BDPA molecules were dissolved in ethanol (99.99% Fisher Scientific) in a concentration of 0.04% by weight. The PDMS stamp had a pattern of an array of circles with diameter of around 1 μm and spacing of 4 μm, and the size of the stamp was around 10 mm $\times$ 10 mm. The stamp was first immersed into the BDPA solution for a minute to ink its surface. Then the stamp was briefly rinsed with deionised water and dried in a stream of nitrogen gas to remove excess solution. The stamp was then pressed to form a conformal contact with the freshly cleaved graphite surface for 5 seconds to print the molecules onto the surface. Before doing this, this procedure was carried out using pure ethanol (i.e. no molecules), and it was verified that no observable pattern of any kind was transferred to the surface.

From the SEM image in Figure 8(a), we can see that a large area of the graphite surface is covered with the array of circles of BDPA. In fact, an area of more than 4 mm $\times$ 4 mm area was printed with BDPA. The size and the spacing of the circles conform to the patterns on the stamp. If we look closer as in Figure 8(b), the BDPA molecules form an array of circles, though their shapes are not particularly regular and their morphologies are uneven. The BDPA molecules aggregate to form clusters. The line profile across one of these circles shows that the thickness of the circle is around 6.89 nm (Fig. 8(b)), which is significantly thicker than a monolayer. We have attempted to make the circles thinner by using a solution with a lower concentration (0.025% in weight), however, the molecules again tended to diffuse and aggregate together to form clusters rather than wetting the surface to form a monolayer (Fig. 8(c)), most likely due to the hydrophobicity of graphite. This behaviour is similar to the case of evaporation on graphite where the molecules move around and aggregate together to form large islands. The problem of aggregation is exacerbated in the case of microcontact printing because solvent is involved which enhances the molecular mobility.

Our experimental results demonstrate that microcontact printing can transfer a predetermined pattern of the

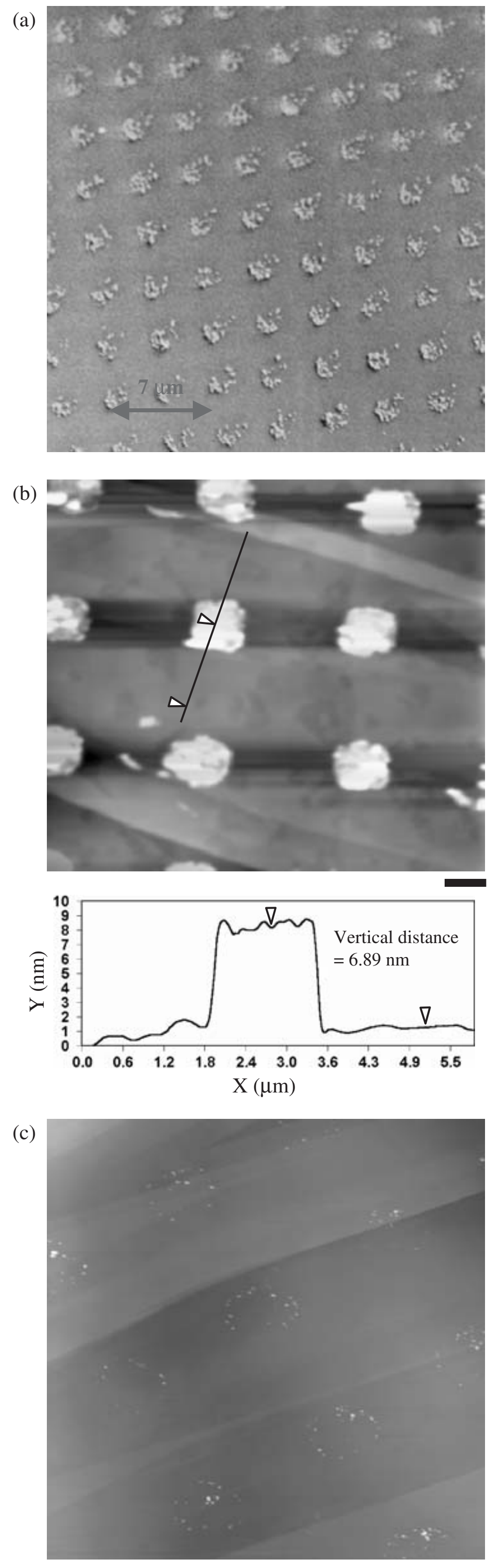

Fig. 8. (a) The SEM image of the microcontact printed HOPG surface with an array of circles of BDPA molecules. (b) The AFM tapping mode image of the microcontact printed HOPG surface, 12 μm $\times$ 12 μm. Scale bar = 1 μm. (c) Microcontact printing of BDPA with a lower concentration solution onto HOPG surface, 12 μm $\times$ 12 μm. AFM tapping mode image. Scale bar = 1 μm.

(a)

(b)

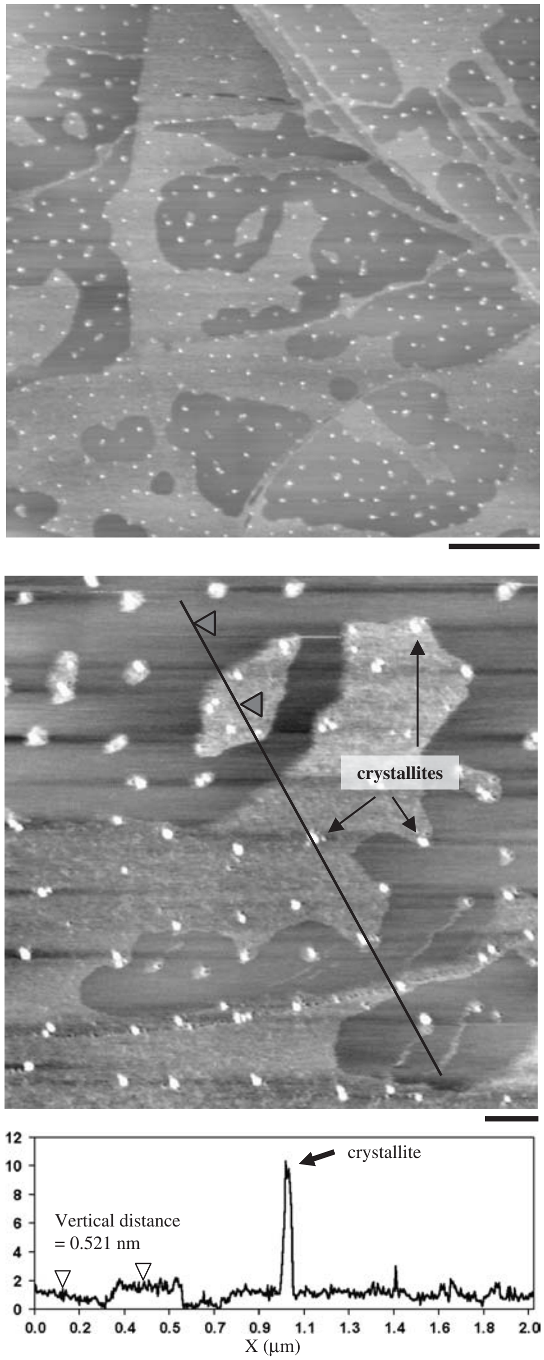

Fig. 9. (a) AFM tapping mode image on the BDPA islands deposited onto HOPG by solvent deposition, 6 μm $\times$ 6 μm. Scale bar = 1 μm. (b) AFM tapping mode image on the same surface as in Figure 9(a), 2 μm $\times$ 2 μm. The line profile shows the thickness of the islands and the clusters. Scale bar = 20 nm.

free-radical organic molecules BDPA onto a substrate, providing a possible route towards experiments on chemical analysis by spin detection with the STM.

2.3. Solvent Deposition

Solvent deposition is one of the most commonly used deposition methods in SPM experiments, especially for biological species like DNA, proteins, and other organic molecules. Organic solvents such as methanol, ethanol, and toluene are suitable for dissolving organic molecules, and some biological samples can be dispersed in pure water. In order to make the deposition as uniform as possible, spin coating is sometimes applied to disperse the material in a more even manner after drop casting. This deposition method has the advantages that it is easy to implement, does not require a complicated experimental set-up, and is applicable to a wide variety of samples. In our experiment, ethanol (99.99% Fisher Scientific, according to the specification, the 0.01% impurity is mostly other solvents, and no residue is detected after evaporation) was used as the solvent for BDPA molecules and the solution concentration was 0.0033% by weight. Drop casting with a micropipette and spin coating were applied to deposit the BDPA molecules onto a freshly cleaved graphite surface. We subsequently imaged the sample surface with the AFM in tapping mode.

Similar to the case of evaporation, the BDPA molecules tend to diffuse on the graphite surface, forming islands ranging in size from around a few hundred nanometers to a micrometer and decorating the step edges (Figs. 9(a) and 9(b)). The molecules, similar to their behaviour on the graphite deposited by evaporation, incline to move around until they either attach to other molecules or obtain stability at the step edges. However, on top of the islands, there are several clusters with the size of around 100 nm $\times$ 100 nm scattered on the surface. If we look at the line profile (Fig. 9(b)), the thickness of the island is around 0.52 nm which is a monolayer, and it shows that the method of solvent deposition can deposit the BDPA free radicals with monolayer thickness onto the substrate. Nevertheless, the aggregates have a height of 8–9 nm which is relatively large. The conjugated bonding structures in the hexagonal and pentagonal rings of BDPA form relatively large electron clouds which will induce strong intermolecular interactions. These aggregates are most likely to be due to Stranski-Krastanov growth (i.e., a monolayer followed by 3D crystallite growth), which has been reported before on HOPG.[24, 25] On a cautionary but obvious note, there is little point in attempting to deposit molecules from a solution with a molecular concentration lower than x% where x is the percentage of *solid* impurities present in the solvent. Even though we deposited using a solution of molecules where their concentration (0.0033%) was 3 times lower than the stated purity of the solvent, the percentage of solid impurities in the solvent was orders of magnitude lower than 0.001%.

3. DISCUSSION

In this work, we have used thermal evaporation, microcontact printing, and solvent deposition methods to deposit free radical organic molecules (BDPA) onto a substrate with controlled thickness. Thermal evaporation, which is an *in-situ* sample preparation method for ultrahigh vacuum experiments, can deposit a submonolayer of BDPA without destroying their spin, and thus it is a feasible way to do the deposition for single electron spin detection experiments. This method has the advantage that it eliminates the problem of aggregation or residue. However, for some free radical organic molecules like TEMPO[26] whose melting points are relatively low (37 °C for TEMPO), it would be difficult to control their evaporation rates for depositing a submonolayer. In these cases, the solvent deposition method is more suitable. From the deposition results on graphite and on gold by evaporation, it is clear that the substrate plays an important role in determining the deposition result. It is interesting to notice that the behaviour of the BDPA on graphite surfaces is essentially independent of the deposition method used. However we can control the influence of such behaviour on the deposition result by avoiding the involvement of the solvent, as shown by the deposition results of evaporation and solvent deposition. The microcontact printing technique has successfully printed the BDPA free radicals with the pattern of an array of circles onto a graphite surface over a large area. While these latter samples are unsuitable for STM experiments, it is possible to make organic spintronics devices by patterning these free radical organic molecules into desired structures by such a patterning technique.

The solvent deposition method can deposit a monolayer of BDPA onto the substrate. This method is particularly useful for free radical organic molecules with low melting points. The aggregation of organic molecules may present a problem to solvent deposition, but the deposition results can be optimised by trying different kinds of solvents, for instance methanol, isopropanol, toluene, and chloroform. It is not impossible to perform solvent deposition *in-situ*. A high-speed solenoid pulse valve[27] can inject the solution towards the substrate under the UHV environment when the valve is opened for a few milliseconds.[28,29] However, the uniformity of the deposition on a substrate is not guaranteed. For free radical organic molecules with poor solubilities, we can use thermal evaporation for deposition.

4. CONCLUSION

The possibilities of a variety of deposition methods for sample preparation for single electron spin detection with the STM were explored. Thermal evaporation, microcontact printing, and solvent deposition can controllably deposit the free radical organic molecules BDPA onto the substrate. Each deposition method has its own pros and cons, and physical properties such as the melting point and solubility of the free radical organic molecules will determine which method to use. The results of this work provide information for the preparation of samples with free radical organic molecules, which will be suitable for, among other things, experiments on probing single spins. We will report on this in later publications.

Acknowledgments: The authors are grateful for research funding from the European Union IST project "QIDPPF–ROSES."

References and Notes

1. R. Wiesendanger, H.-J. Güntherodt, G. Güntherodt, R. J. Gambino, and R. Ruf, *Phys. Rev. Lett.* 65, 247 (**1990**).
2. O. Pietzsch, A. Kubetzka, M. Bode, and R. Wiesendanger, *Appl. Phys. A* 78, 781 (**2004**).
3. S. Heinze, M. Bode, A. Kubetzka, O. Pietzsch, X. Nie, S. Blügel, and R. Wiesendanger, *Science* 288, 1805 (**2000**).
4. Y. Manassen, R. J. Hamers, J. E. Demuth, and A. J. Castellano, Jr., *Phys. Rev. Lett.* 62, 2531 (**1989**).
5. C. Durkan and M. E. Welland, *Appl. Phys. Lett.* 80, 458 (**2002**).
6. A study confirming our STM noise spectroscopy findings on BDPA has been submitted for publication by an independent group (Y. Manassen, private communication).
7. W. T. Pong and C. Durkan, *Proceedings of the 5th International Conference 7th Annual General Meeting of the European Society for Precision Engineering and Nanotechnology*, Montpellier, France (**2005**), Vol. 1, p. 241.
8. C. Durkan, *Contemporary Physics* 45, 1 (**2004**).
9. Molecular weight 496.6, CAS number 35585-94-5, purchased from Sigma-Aldrich.
10. G. Wagoner, *Phys. Rev.* 118, 647 (**1960**).
11. F. J. Dyson, *Phys. Rev.* 98, 349 (**1955**); P. Burgardt and M. S. Seehra, *Phys. Rev. B* 16, 1802 (**1977**).
12. A. Jánossy, F. Simon, T. Fehér, A. Rockenbauer, L. Korecz, C. Chen, A. J. S. Chowdhury, and J. W. Hodby, *Phys. Rev. B* 59, 1176 (**1999**).
13. R. Emch, J. Nogami, M. M. Dovek, C. A. Lang, and C. F. Quate, *J. Appl. Phys.* 65, 79 (**1989**).
14. Z. H. Wang and M. Moskovits, *J. Appl. Phys.* 71, 5401 (**1992**).
15. J. Kim, H. Uchida, K. Yoshida, H. Kim, K. Nishimura, and M. Inoue, *Jpn. J. Appl. Phys.* 42, 3616 (**2003**).
16. Q. Guo, F. Yin, and R. Palmer, *Small* 1, 76 (**2005**).
17. M. Schunack, F. Rosei, Y. Naitoh, P. Jiang, A. Gourdon, E. Lægsgaard, I. Stensgaard, C. Joachim, and F. Besenbacher, *J. Chem. Phys.* 117, 6259 (**2002**).
18. H. Li, D. J. Kang, M. G. Blamire, and W. T. S. Huck, *Nano Lett.* 2, 347 (**2002**).
19. A. Bernard, E. Delamarche, H. Schmid, B. Michel, H. R. Bosshard, and H. Biebuyck, *Langmuir* 14, 2225 (**1998**).
20. N. L. Jeon, I. S. Choi, G. M. Whitesides, N. Y. Kim, P. E. Laibinis, Y. Harada, K. R. Finnie, G. S. Girolami, and R. G. Nuzzo, *Appl. Phys. Lett.* 76, 4201 (**1999**).
21. H. X. He, Q. G. Li, Z. Y. Zhou, H. Zhang, S. F. Y. Li, and Z. F. Liu, *Langmuir* 16, 9683 (**2000**).
22. T. L. Breen, P. M. Fryer, R. W. Nunes, and M. E. Rothwell, *Langmuir* 18, 194 (**2002**).
23. Y. Koide, Q. Wang, J. Cui, D. D. Benson, and T. J. Marks, *J. Am. Chem. Soc.* 122, 266 (**2000**).
24. M. Lackinger, S. Griessl, W. M. Heckl, and M. Hietschold, *Anal. Bioanal. Chem.* 374, 675 (**2002**).
25. B. Daudin, F. Widmann, G. Feuillet, Y. Samson, M. Arlery, and J. L. Rouviére, *Phys. Rev. B* 56, R7069 (**1997**).
26. Molecular weight 156.2, CAS number 2564-83-2, available from Sigma-Aldrich.
27. General Valve Co., Series 9.
28. H. Tanaka and T. Kawai, *J. Vac. Sci. Technol. B* 15, 602 (**1997**).
29. C. Hamai, H. Tanaka, and T. Kawai, *J. Vac. Sci. Technol. B* 17, 1313 (**1999**).

Received: 25 July 2006. Revised/Accepted: 31 August 2006.